Use of Particle Filtering in RSSI-Based Localization by Drone Base Stations

Serife Senem Karaman
TOBB Univ. of Econ. and Technology
Dept. of Electrical and Electronics Eng.
06560, Ankara, Turkey
skaraman@etu.edu.tr

Alper Akarsu
Havelsan Inc.
Mustafa Kemal Mah. 2120 Cad. No:39
06510, Ankara, Turkey
aakarsu@etu.edu.tr

Tolga Girici
TOBB Univ. of Econ. and Technology
Dept. of Electrical and Electronics Eng.
06560, Ankara, Turkey
tgirici@etu.edu.tr

***Abstract*—Drone Base Stations (DBSs) provide flexible deployment and line-of-sight coverage opportunities, which led to many use cases, such as broadband Internet, military, surveillance, agriculture etc. DBSs can optimize and adapt their positions based on user location information. Especially in GPS-denied tactical scenarios ground user location estimation is an important problem. In this work we investigate particle filter as a method of user position estimation. We utilize the recently proposed air-to-ground pathloss model for RSSI-based location estimation. We investigate different DBS trajectories and various resampling methods. Finally, we show by simulations that particle filtering performs comparably to maximum likelihood estimation, which makes it a suitable alternative for localization and tracking.**

***Index Terms*—Localization, drone base stations, UAV estimation, particle filter, tracking**

I. Introduction

Drone technology significantly enhanced in the last 10-15 years. Advancements in the materials technology, chipsets and software significantly improved the capability of drones. This led to many novel applications of drones such as, Internet of Things, Surveillance, Military, Broadband Internet Access, drone-based delivery etc. Main limitations of drones are their battery limit. In the case of broadband wireless access, the requirement of a wireless backhaul is another limitation. Main advantage of drones is their mobility. Their position can be optimized for maximum coverage or throughput. Another advantage is that it's more possible to provide a line-of-sight (LoS) connection because of their altitude. Due to these advantages, use of drones as base stations in wireless access has gained popularity as a research topic in the last five years. The objective of these studies are either to maximize drone coverage or maximize the total throughput. Most of these studies are based on the air-to-ground channel model proposed in [1]. The same author investigated the optimal altitude of drone for maximum coverage [2]. 3D placement of a drone was studied in [3], [4]. We previously proposed a method that jointly optimizes the drone placement and the number of drones for maximum fair throughput [5].

All of the studies mentioned above implicitly assume that the locations of the ground nodes are perfectly known. If both the drone and the nodes have GPS capability, then this is a reasonable assumption. However, this assumption may not always be realistic. In tactical/military scenarios GPS may be blocked. Moreover, the ground node may just be simple sensor nodes that cannot contain GPS modules. In such cases, RSSI-based ground node location estimation is a promising alternative. The air-to-ground channel model in [1] can be used to estimate the node locations based on pathloss measurements. The authors in [6] and [7] are the first ones that propose such a method for drone base stations.

RSSI-based localization has been previously considered for indoor wireless sensor networks [8]. The authors in [9] extended this for an aerial mobile robot (beacon). In [9] particle filtering method was utilized to estimate the location of a ground node. In that work the authors used a different, much simpler pathloss model. In this work our goal is to investigate the use of particle filtering that utilizes the channel model in [1]. We will investigate the optimal drone altitude, number of particles, number of iterations and trajectory on the estimation performance. We will also investigate the effects of different resampling schemes on the performance. We will also compare the performance of particle filtering with that of the maximum likelihood estimation.

II. System Model

We consider a single DBS that estimates the location of a single ground node. Same estimation can be easily repeated for multiple nodes. The node is located randomly in a square area of size D_{max}. The position of the node is denoted by (x^u, y^u) and the location of the DBS is denoted by (x^d, y^d, h^d). The parameter r^{ud} denotes the horizontal distance $r^{ud} = \sqrt{(x^u - x^d)^2 + (y^u - y^d)^2}$ between the node and DBS. The actual distance can be computed by $d^{ud} = \sqrt{(h^d)^2 + (r^{ud})^2}$. The elevation angle is defined as $\theta^{ud} = \arctan\left(\frac{h^d}{r^{ud}}\right)$. We assume a probabilistic pathloss model originally proposed in [1] and [2]. According to this model, the probability of line-of-sight (LoS) and non-line-of-sight (NLoS) between DBS and node depends on the elevation angle θ^{ud}.

$$p^{ud}_{LoS}(\theta^{ud}) = \frac{1}{1 + a(-b(\frac{180}{\pi}\arctan(\frac{h^d}{r^{ud}}) - a))}$$
$$p^{ud}_{NLoS}(\theta^{ud}) = 1 - p^{ud}_{LoS} \quad (1)$$

978-1-7281-1244-2/19/$ 31.00 ©2019 IEEE

Here a and b are environmental parameters, which differ according to the deployment scenario (urban, suburban, rural etc.). For the LoS and NLoS cases, path losses (in dB's) are defined respectively as follows,

$$PL_{LoS}^{ud} = 10\gamma \log\left(\frac{4\pi d^{ud} f_c}{c}\right) + \eta_{LoS}(\theta^{ud})$$
$$PL_{NLoS}^{ud} = 10\gamma \log\left(\frac{4\pi d^{ud} f_c}{c}\right) + \eta_{NLoS}(\theta^{ud}) \quad (2)$$

Here γ is the pathloss exponent, f_c is the carrier frequency (Hz), c is the speed of light (m/s). Parameters η_{LoS} and η_{NLoS} are the excess pathlosses for the LoS and NLoS cases, respectively.

In [1] pathloss samples are fitted to a Gaussian random distribution, as a function of the elevation angle.

$$\eta_{LoS}(\theta^{ud}) \sim \quad \mathcal{N}(\mu_{LoS}, \sigma_{LoS}^2(\theta^{ud}))$$
$$\eta_{NLoS}(\theta^{ud}) \sim \quad \mathcal{N}(\mu_{NLoS}, \sigma_{NLoS}^2(\theta^{ud})) \quad (3)$$

where μ_{LoS} and μ_{NLoS} are the mean and $\sigma_{LoS}(\theta^{ud})$ and $\sigma_{NLoS}(\theta^{ud})$ are the standard deviations of the excess losses for the LoS and NLoS cases, respectively.

$$\sigma_{LoS}(\theta^{ud}) = \quad \alpha_1 \exp(-\beta_1 \theta^{ud})$$
$$\sigma_{NLoS}(\theta^{ud}) = \quad \alpha_2 \exp(-\beta_2 \theta^{ud}) \quad (4)$$

where $\alpha_1, \alpha_2, \beta_1, \beta_2$ are scenario-dependent parameters.

Mean value of the pathloss for the LoS and NLoS cases, depending on the elevation angle and distance is formulated as follows,

$$\overline{PL}_{LoS}(\theta^{ud}, d^{ud}) = \quad 10\gamma \log\left(\frac{4\pi d^{ud} f_c}{c}\right) + \mu_{LoS}$$
$$\overline{PL}_{NLoS}(\theta^{ud}, d^{ud}) = \quad 10\gamma \log\left(\frac{4\pi d^{ud} f_c}{c}\right) + \mu_{NLoS} \quad (5)$$

Probability density function of the pathloss, given the elevation angle and distance is formulated as follows,

$$f_{PL}(pl|\theta^{ud}, d^{ud}) = \frac{p_{LoS}^{ud}(\theta^{ud})}{\sqrt{2\pi\sigma_{LoS}^2(\theta^{ud})}} e^{\frac{-(pl-\overline{PL}_{LoS}(\theta^{ud}, d^{ud}))^2}{2\sigma_{LoS}^2(\theta^{ud})}}$$
$$+ \frac{p_{NLoS}^{ud}(\theta^{ud})}{\sqrt{2\pi\sigma_{NLoS}^2(\theta^{ud})}} e^{\frac{-(pl-\overline{PL}_{NLoS}(\theta^{ud}, d^{ud}))^2}{2\sigma_{NLoS}^2(\theta^{ud})}} \quad (6)$$

Table I shows the pathloss parameter values used in this paper. These are typical urban pathloss parameters.

TABLE I
CHANNEL AND PATHLOSS PARAMETERS (URBAN SCENARIO)

Parameter	Definition	Value
f_c	Carrier Frequency	$2GHz$
c	Speed of light	3×10^8 m/s
D_{max}	Area size	$2000m$
a, b	Environmental Parameters	9.61, 0.16
α_1, β_1	LoS Parameters	10.39, 0.05
α_2, β_2	NLoS Parameters	29.6, 0.03
μ_{LoS}, μ_{NLoS}	Mean Excess Path loss	$1dB$, $20dB$

Algorithm 1 Particle Filter Algorithm

1: Initialize L particle positions: $(x^l, y^l), \forall l = 1, ..., L, t = 0$, $w_l = \frac{1}{L}, \forall 1, ..., L$.
2: Calculate θ^{ld} and $d^{ld}, \forall l = 1, ..., L$.
3: $N_{th} = 0.1L$.
4: **while** not `converge` **do**
5: $t = t + 1$
6: Perform pathloss measurement: pl_t.
7: Calculate: $f_{PL}(pl_t|\theta^{ld}, d^{ld}), \forall l = 1, ..., L$.
8: Update weights: $w_l = w_l \times f_{PL}(pl_t|\theta^{ld}, d^{ld}), \forall l = 1, ..., L$.
9: Normalize weights: $w_l \rightarrow \frac{w_l}{\sum_{i=1}^{L} w_i}, \forall l = 1, ..., L$.
10: Calculate: $N_{eff} = \frac{1}{\sum_{l=1}^{L} w_l^2}$.
11: **if** $N_{eff} < N_{th}$ **then**
12: Perform `resampling`: $(x^l, y^l), \forall l = 1, ..., L$.
13: Reset the weights: $w_l = \frac{1}{L}, \forall 1, ..., L$.
14: **end if**
15: Random perturbation: $(x^l, y^l) \rightarrow (x^l + \texttt{rand} \times \Delta_x, y^l + \texttt{rand} \times \Delta_y), \forall l = 1, ..., L$.
16: Calculate θ^{ld} and $d^{ld}, \forall l = 1, ..., L$.
17: Estimation update: $(\mu_x, \mu_y) = \left(\sum_{l=1}^{L} w_l x^l, \sum_{l=1}^{L} w_l y^l\right)$
18: Variance update: $(\sigma_x^2, \sigma_y^2) = \left(\sum_{l=1}^{L} (x^l - \mu_x)^2 w_l, \sum_{l=1}^{L} (y^l - \mu_y)^2 w_l\right), \forall l = 1, ..., L$.
19: **if** $(\sigma_x < \sigma_{th})$ and $(\sigma_y < \sigma_{th})$ **then**
20: `converge`.
21: **end if**
22: **end while**
23: **Return**: (μ_x, μ_y).

III. LOCATION ESTIMATION USING PARTICLE FILTER

In [9] particle filtering is used by an aerial robot in order to locate a ground node. In our work there is a single DBS that follows a trajectory and makes pathloss measurements at regulary spaced points on the trajectory.

The algorithm initializes L particle positions randomly on a square area of size D_{max}. Particle weights are initialized to $\frac{1}{L}$ (Line 1). The DBS is assumed to perfectly know its position. Elevation angle and distance for each particle to the DBS is calculated (Line 2). Effective particle size is denoted by N_{th} and it is used to trigger resampling. It is chosen as $N_{th} = 0.1L$ based on [9], [10] (Line 3). Main loop is in Lines 4-22. At each step, the DBS makes a pathloss measurement (Line 6) and calculates the likelihood of the measured pathloss for each particle (Line 7). Weights are updated and normalized in Lines 8,9. Effective particle size is calculated and if it falls below the threshold, then resampling is triggered (Lines 10-14). As will be explained later, resampling results in cloning

of the particles with higher likelihood. Therefore they are randomly perturbed in Lines 15-16 in order to differentiate their positions. Estimation is the weighted sum of particle positions. Estimation (mean) and variance of particle positions are calculated in Lines 17,18. If the variance falls below a threshold then the algorithm is terminated.

A. Simulations

In this part we aim to determine suitable values for the number of particles (L), radius of the DBS trajectory (r) and DBS altitude (h). We used the pathloss parameters in Table I and each time varied one of the parameters and kept the others fixed. Results are presented in Table II. The first two rows show that an altitude of $h = 800$m is enough for a good estimation performance. The next two rows show that a radius of $\frac{D_{max}}{3}$ is optimal. Finally the last two rows show that $L = 500$ particles are enough for a good estimation performance. In the following simulations we will use these parameter values.

IV. Resampling Methods

In resampling, particles are regenerated based on the previous particle weights. This is done in order to elimine low-weight (i.e. low likelihood) particles. Some resampling methods are described as follows,

- Multinomial Resampling: First, let us define $Q_t^m = \sum_{l=1}^{m} w_m$. In this method, first a random number is generated according to $u \sim U(0,1)$. Then the particle w_l such that $Q_t^{l-1} < u \leq Q_t^l$ is selected as the sample. This procedure is repeated L times.
- Residual Resampling: This method consists of two stages. In the first stage the particles with weight greater than $\frac{1}{L}$ are deterministically resampled. Such a particle l is resampled $N_l = \lfloor L \times w_l \rfloor$ times. There remains $L - \sum_{l=1}^{L} N_l$ resamplings. For the second stage, each weight is updated as $w_l - \frac{N_l}{L}$. Second stage of resampling is performed with these weight using the multinomial resampling methods.
- Stratified Resampling: This method divides the $(0,1)$ interval to L equal subintervals like $(0, 1/L] \cup ... \cup (1 - 1/L, 1]$. A random number is generated in each subinterval, where $u^n \sim U(\frac{n-1}{L}, \frac{n}{L}), n = 1, ..., L$. For each u^n, the particle w_l satisfying $Q_t^{l-1} < u^n \leq Q_t^l$ is selected as the sample.
- Systematic Resampling: In this method the first random number is distributed as $u^1 \sim (0, 1/L]$. The rest of the numbers are determined deterministically as $u^n = u^1 + \frac{n-1}{L}, n = 2, 3, ..., L$. For each u^n, the particle w_l satisfying $Q_t^{l-1} < u^n \leq Q_t^l$ is selected as the sample.

Stratified and Systematic methods have usually less complexity $O(L)$ [11]. Systematic requires less random number generations, which is also good for complexity.

In this part we compare these four resampling methods. We consider a square area of size 2000 meters. A ground node is placed randomly on this area. The DBS is at altitude 800 meters and follows a circular trajectory with a radius of $R = \frac{2000}{3}$ meters. It applies the particle filtering for a fixed T steps, where it makes a pathloss measurement at T equispaced points on the circular trajectory. We consider $T = 10, 15, ..., 35, 40$. We use $L = 500$ particles. For the random perturbation we use $\Delta_x = \Delta_y = 0.1 \times \frac{2000}{\sqrt{500}}$. We don't use the threshold σ_{th}; instead we apply the PF for fixed T steps. We assume that these T locations are sufficiently apart so that the pathloss measurements are independent. We perform 100 independent experiments, where the ground node is positioned randomly each time. Table III shows the mean localization error in 100 experiments. As expected, the localization error tends to decreases as the number of pathloss measurements increase. Results show that the four methods do not differ significantly in terms of the mean error. Multinomial , Stratified and Systematic resampling seem to bet slightly better than the Stratified Resampling.

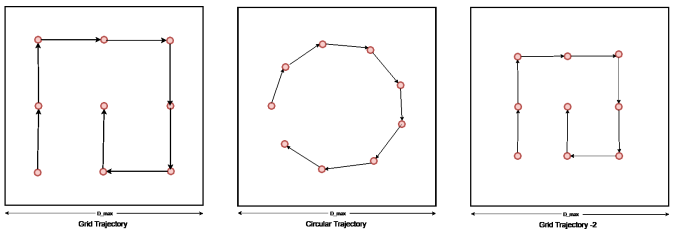

Fig. 1. Grid and Circular trajectories for $T = 9$. The last trajectory requires the same energy as the circular one.

Table IV shows the maximum (in 100 experiments) of the localization errors for the four resampling methods. Maximum error seems to be more volatile, when compared to the mean error. Here the systematic method is the best in 4 of the 7 cases. It is significantly better than the other resampling methods in terms of maximum error. This result more or less agrees with the one in [11]. Therefore, from this point on we will continue with the systematic resampling method.

V. Comparison of Trajectories

A. Energy Expenditure Model

DBSs are battery-limited devices, therefore they have to operate in an energy-efficient manner. The drone can spend more time in order to travel more and make more pathloss measurements, however this would drain its battery. In this part we will compare different types of trajectories in particle-filter based location estimation. We neglect the energy spent for communication and focus on the propulsion energy. We use the UAV energy that was originally proposed in [12] and used in [13]. Energy consumption consists of the energy required to turn the rotor blade (blade profile), energy required to overcome the drag force (parasitic power) and the energy required to induced drag of lift creation (induced power). The total power consumption (as a function of speed v) can be written as,

$$P_d(v) = mgv_{ind} + \frac{1}{2}\rho v^3 C_{ds} + k_0(1 + 3\frac{v^2}{v_t^2}) \qquad (7)$$

$L=1000, T=12, r=\frac{2000}{3}, h=...$	200	400	600	800	1000	1200	1400
Mean error vs h	363	197	126	105	103	102	110
$L=1000, T=12, h=500, r=...$	$\frac{2000}{2}$	$\frac{2000}{3}$	$\frac{2000}{4}$	$\frac{2000}{5}$	$\frac{2000}{6}$	$\frac{2000}{7}$	$\frac{2000}{8}$
Mean error vs. r	165	133	159	183	242	261	336
$h=800, T=12, r=\frac{2000}{3}, L=...$	100	500	1000	1500	2000	2500	3000
Mean error vs L	139	96	105	97	113	96	109

TABLE II

MEAN ESTIMATION ERROR (M) VERSUS, NUMBER OF PARTICLES, DBS ALTITUDE AND RADIUS OF THE DBS TRAJECTORY

	Multinomial	Residual	Stratified	Systematic
T=10	106	128	106	118
T=15	97	97	98	98
T=20	88	77	88	80
T=25	67	68	68	68
T=30	68	68	67	63
T=35	60	60	60	55
T=40	56	61	55	63

TABLE III

MEAN LOCALIZATION ERROR FOR FOUR RESAMPLING METHODS.

	Multinomial	Residual	Stratified	Systematic
T=10	450	445	461	445
T=15	395	445	397	331
T=20	285	234	389	232
T=25	213	213	210	268
T=30	196	212	187	206
T=35	190	202	232	164
T=40	224	205	174	203

TABLE IV

MAXIMUM LOCALIZATION ERROR FOR FOUR RESAMPLING METHODS.

The three terms are the induced, parasitic and blade profile components, respectively. Here m is the DBS mass, g is the gravity, ρ is the air density, v_t is the tip speed of the rotor blade and C_{ds} and k_0 are constants. Typical values of these parameters are 5 kg, $10m/sec^2$, 1.225, 100, 0.4 and 570 , respectively. Mean induced velocity v_{ind} is,

$$v_{ind} = \sqrt{\frac{-v^2 + \sqrt{v^4 + (\frac{mg}{\rho A_d})^2}}{2}} \tag{8}$$

where A_d is the area of the UAV, which is taken as $0.25m^2$. In [13] is is assumed that the DBS hovers ($v = 0$) for 5 seconds during pathloss measurement. In that case the power expenditure becomes $P_d(0) = k_0 + \sqrt{\frac{(mg)^3}{2\rho A_d}}$. It is found that such a drone achieves the least energy expenditure at a speed of 40 km/h. We assume that the DBS follows the straight line between the trajectory points (with speed 40 km/h) and hovers for 5 seconds at each point.

We only consider $T = 4, 9, 16, 25$ (i.e. square integer numbers). With this choice, we can divide the square area into equal grids. Figure 1 shows the trajectories considered for $T = 9$. Three types of trajectories are compared,

- Grid Trajectory: The area is divided into equal grids. Each hovering point is in the middle of a grid. Total energy expenditure approximately becomes,

$$E_T \simeq \frac{T-1}{40} \times \frac{D_{max}}{3} P_d(40) + T \times P(0) \tag{9}$$

	T=4	T=9	T=16	T=25
Grid Traj. Energy	3.29×10^5	5.97×10^5	8.60×10^5	11.3×10^5
Circ. Traj. Energy	3.12×10^5	4.26×10^5	4.96×10^5	5.64×10^5
Grid Traj. Error	262	147	87	70
Circ. Traj. Error	248	120	82	66
Grid Traj. Max Error	1515	459	236	186
Circ. Traj. Max Error	1208	399	224	194

TABLE V

COMPARISON OF LOCALIZATION ERROR AND ENERGY EXPENDITURE FOR GRID AND CIRCULAR TRAJECTORIES.

- Circular Trajectory: The DBS travels on a circle of radius $R = \frac{D_{max}}{3}$. As shown in the middle figure in Fig. 1 it hovers and measures the pathloss at T equispaced points on the trajectory. Total energy expenditure approximately becomes,

$$E_T \simeq \frac{T-1}{40} \times \sqrt{2}R\sqrt{1 - \cos\left(\frac{2\pi}{T}\right)} P_d(40) + T \times P(0) \tag{10}$$

, where R is the radius of the circular trajectory. The two terms of the above equation are the forward flight energy and the hovering energy, respectively.
- Grid Trajectory - 2: In this trajectory the hovering points are located on a grid, but the points are closer to the center. This trajectory spends an energy equal to the circular trajectory.

Table V presents the energy expenditures and mean localization errors for the grid and circular trajectories. Results reveal that error performance of the grid trajectory tends to get better as T increases. However it's energy expenditure is significantly higher than the circular trajectory. Grid trajectory draws a spiral to the center of the area and it results in greater distance of forward flight.

In order for a fair comparison, we considered the Grid Trajectory -2, which results in equal energy with the circular trajectory. We did the computations for $T = 16$ and saw that both trajectory spend 4.96×10^5 J's of energy. Mean error for the circular trajectory is 67.9 meters and the mean error for the Grid Trajectory - 2 is 84 meters. This shows that under the same energy expenditure circular trajectory is better than the grid trajectory. Grid trajectory spans the area more uniformly, but it travels much more distance in order to do that.

VI. COMPARISON WITH THE MAXIMUM LIKELIHOOD ESTIMATION

This is a preliminary work that investigates the use of particle filter for RSSI-based node location estimation for the

air-to-ground channel model. Particle filter will be especially useful for tracking a mobile ground node, which will be a future work. However, for a *fixed* ground node, maximum likelihood estimation can also be formulated. In fact, it was formulated in [14]. In this part, we will compare the error performances of the particle filter and maximum likelihood estimation. Maximum likelihood estimator can be formulated as follow,

$$(\widehat{x}^u, \widehat{y}^u) = \max_{x^u, y^u} \prod_{t=1}^{T} f_{PL}(pl_t | \theta_t^{ud}, d_t^{ud}) \tag{11}$$

Here $f_{PL}(pl_t|\theta_t^{ud}, d_t^{ud})$ defined in Eq. (6) is the probability density function of pathloss given the elevation angle and distance. $pl_t, t = 1, 2, ..., T$ are the pathloss measurements at the trajectory points.

Table VI shows the comparison of the particle filtering with maximum likelihood estimator. Circular trajectory is used with radius equal to $D_{max}/3$ and altitude is 800 m. Systematic resampling is used in the particle filtering. 100 random trials are performed and the table shows the mean error and maximum error in 100 trials. Results show that mean error of PD is very close to the MLE. In terms of the maximum error, the results are more interesting. The maximum error in 100 trials is much better with PF than the MLE. More detailed simulations will be done as future work.

	PF (Mean)	MLE (Mean)	PF (Max)	MLE (Max)
T=10	117	119	445	858
T=15	98	93	331	242
T=20	80	80	232	360
T=25	68	73	268	444
T=30	62	64	206	425
T=35	55	56	164	345
T=40	62	50	204	253

TABLE VI
COMPARISON OF PARTICLE FILTERING WITH MAXIMUM LIKELIHOOD ESTIMATION. SYSTEMATIC RESAMPLING IS USED IN PARTICLE FILTERING.

VII. CONCLUSIONS AND FUTURE WORK

Drone base stations (DBS) are becoming popular with many applications such as military, surveillance or Internet of Things. In GPS-denied scenarios, the DBS should be able to estimate the locations of the ground nodes and track them if they are mobile. This is a preliminary work that studies particle filtering as localization method for a ground node. Four resampling methods for the particle filtering are compared. Systematic resampling turned out to be the best among them. Simulations are carried out in order to determine the optimal trajectory of the DBS. Results reveal that, for the same energy expenditure, circular trajectory results in better error performance than the grid trajectory. Finally particle filtering is compared to maximum likelihood estimation. Results show that particle filtering has a performance comparable to the maximum likelihood estimation.

Future work will address tracking of a *mobile* user. Particle filtering is a good candidate for mobile tracking. A good tracking performance would involve calibration of the number of particles, random perturbation along with the resampling method. Energy-efficiency is also an important factor in maximizing the battery duration and maximizing the tracking time. Therefore, the speed of the DBS should also be optimized.

REFERENCES

[1] A. Al-Hourani, S. Kandeepan, and A. Jamalipour, "Modeling air-to-ground path loss for low altitude platforms in urban environments," in *Global Communications Conference (GLOBECOM), 2014 IEEE*. IEEE, 2014, pp. 2898–2904.

[2] A. Al-Hourani, S. Kandeepan, and S. Lardner, "Optimal lap altitude for maximum coverage," *IEEE Wireless Communications Letters*, vol. 3, no. 6, pp. 569–572, 2014.

[3] R. I. Bor-Yaliniz, A. El-Keyi, and H. Yanikomeroglu, "Efficient 3-d placement of an aerial base station in next generation cellular networks," in *Communications (ICC), 2016 IEEE International Conference on*. IEEE, 2016, pp. 1–5.

[4] M. Alzenad, A. El-Keyi, and H. Yanikomeroglu, "3d placement of an unmanned aerial vehicle base station for maximum coverage of users with different qos requirements," *IEEE Wireless Communications Letters*, 2017.

[5] A. Akarsu and T. Girici, "Fairness aware multiple drone base station deployment," *IET Communications*, vol. 12, no. 4, pp. 425–431, 2017.

[6] ——, "Failure aware deployment of drone base stations," in *Telecommunication Forum (TELFOR), 2018 26th. IEEE, , Sirbia.* IEEE, 2018, pp. 1–5.

[7] A. C. H. Sallouha, M. M. Azari and S. Pollin, "Aerial anchors positioning for reliable rss-based outdoor localization in urban environments," *IEEE Wireless Communications Letters*, 2017.

[8] G. Zanca, F. Zorzi, A. Zanella, and M. Zorzi, "Experimental comparison of rssi-based localization algorithms for indoor wireless sensor networks," in *Proceedings of the workshop on Real-world wireless sensor networks*. ACM, 2008, pp. 1–5.

[9] I. M. F. Caballero, L. Merino and A. Ollero, "A particle filtering method for wireless sensor network localization with an aerial robot beacon," in *International Conference on Robotics and Automation*. IEEE, 2008, pp. 596–601.

[10] S. Thrun, W. Burgard, and D. Fox, *Probabilistic robotics*. MIT press, 2005.

[11] P. Kozierski, M. Lis, and J. Zietkiewicz, "Resampling in particle filtering-comparison," 2013.

[12] A. Filippone, *Flight performance of fixed and rotary wing aircraft*. Elsevier, 2006.

[13] H. Sallouha, M. M. Azari, and S. Pollin, "Energy-constrained uav trajectory design for ground node localization," *arXiv preprint arXiv:1806.02055*, 2018.

[14] A. Akarsu and T. Girici, "Drone base station deployment in urban warfare," *Submitted to, IEEE Transactions on Aerospace and Electronics*, vol. 1, no. 1, pp. 1–14, 2018.